Oceanic Core Complex or not? When partial spreading asymmetry triggers seafloor diversity

Florent Szitkar (florent.szitkar@ngu.no)
The Geological Survey of Norway
Laurent Gernigon
Geological Survey of Norway (NGU) https://orcid.org/0000-0002-4032-0549
Anna Lim
Argeo Survey AS
Marco Brönner
Geological Survey of Norway

Article

Keywords: Oceanic Core Complex, Proto-Core Complexes, tectonics, geophysics

Posted Date: June 22nd, 2021

DOI: https://doi.org/10.21203/rs.3.rs-464587/v1

Abstract

We use high-resolution and regional geophysical data to study a bathymetric high near the Mohns/Knipovich ridges junction, in the Norwegian-Greenland Sea. Near-seafloor magnetic data over hydrothermal site Loki's Castle first support the basaltic nature of the seafloor. We then combine this result with regional magnetic and bathymetric considerations to investigate the crustal architecture in the vicinity of the junction. We show that the spreading asymmetry is insufficient to allow the development of Oceanic Core Complexes. Instead, this atypical off-axis hill is dominantly basaltic and should be interpreted as the first inside corner hogback structure identified along an active mid-ocean ridge system. Our conclusion tempers the definition of Oceanic Core Complex and underlines that bathymetric highs located off axis from slow-spreading centers cannot always be interpreted as such. This intermediate type of spreading paves the way to the introduction of a new class of oceanic structure referred to as Proto-Core Complexes.

1) Introduction

The Norwegian territorial waters host a long extension of mid-ocean ridges, ranging from Iceland to the Gakkel Ridge. The section between the Jan Mayen and the Molloy fracture zones is divided into two spreading segments, known as the Mohns and Knipovich Ridges[1]. At their intersection, the ridges show a bend in the spreading axis direction at 73°.40'N 8°.20'E. Both of them are characterized by slow-spreading rate (< 20 mm/year)[2–5], implying a limited magma budget unable to fully accommodate the oceanic expansion[6–8]. This low magma input results in a dominantly tectonic spreading environment including a complex fault network easing crustal circulation of seawater and favoring hydrothermalism.

Several active and inactive hydrothermal vent fields have been documented in this area, the most notable being the high-temperature hydrothermal site Loki's Castle[9], sitting along the northwestern flank of the Mohns Ridge axis. Based on Honsho et al.[10] Bayesian inversion, we confirm the basaltic nature of the seafloor underneath the site. We then combine this result with regional magnetic and bathymetric observations to discuss the tectonic processes leading to the formation of the prominent but enigmatic hill feature located near the junction between the two ridges (Hill A, Fig. 1a). Despite a partial spreading asymmetry, magnetic inversion and modelling results suggest that the Hill A is dominantly basaltic, and therefore cannot be interpreted as a traditional Oceanic Core Complex (OCC). Its formation should result from incomplete mantle denudation leading to the definition of a specific type of oceanic structure, introduced as Proto-Core Complex, or PCC, in this paper.

2) Results

2.1) Rift setting and survey area

The Mohns and Knipovich Ridges form the northern extension of the Mid-Atlantic Ridge (MAR) and ensure the continuity between the MAR and the Gakkel Ridge. Their junction is associated with a 70°

bend in the ridge axis orientation.

This peculiar spreading ridge configuration is highlighted on the bathymetry[11] and associated ruggedness analysis[12] (Fig. 1a, b). Within the Knipovich Ridge, the axial rift valley shows an "en echelon" system including NNE-trending troughs, approximately 3.5-4 km deep. South of 74°47'N, the strike of these rift troughs becomes progressively N30°E oriented and gradually approaches that of the rift valley (N20°E), in the southern Mohns Ridge segment.

Between the Mohns and Knipovich Ridges, the western slope of the rift valley presents fault benches covered with sediments as thick as 1 km, however seismic and dredging data reveal that the steep slopes are devoid of sediments and made of basaltic pillow lava[13]. The eastern flank of the axial rift valley (rising 500–1000 m above the ridge axis) is considerably lower compared to the western slope (rising 1000–2000 m above the ridge axis), witnessing a spreading asymmetry. West of the rift valley, linear elevated ridges progressively turn from a N30°E orientation to the South to a N10°W orientation to the North. Regional bathymetry also reveals a series of prominent features topping at 600 m below sea level to the Northwest of the ridges junction. The various highs are bordered by steep escarpments showing high ruggedness indexes (Fig. 1a, b). North and East of the Mohns Ridge, the main structural highs pass into the deep structures of the Knipovich Ridge. There occurs a system of wide benches separated by low scarps plunging towards the bending rift valley.

Approximately 25 km southwest of the bending rift valley lies the high-temperature hydrothermal site Loki's Castle (Fig. 1a, 2a). The site stands at 2,350 m depth and is made of two roughly circular mounds, 150–200 m width, actively venting fluids at 310–320°C[9]. As part of the MarMine oceanographic campaign, this site was investigated by R/V *Polar King* in 2016[14]. The ship deployed the Autonomous Underwater Vehicle (AUV) *Hugin*, which carried out a dive over the hydrothermal site to collect high-resolution bathymetric and magnetic data. The near-seafloor magnetic data were acquired by a fluxgate magnetometer from *Ocean Floor Geophysics* mounted to the AUV[15] (Methods and Supplementary Information). The AUV routes were 150 m apart and 100 m above the seafloor (Fig. 2b, c, d).

Airborne aeromagnetic data were also collected in 2016 and 2018, as part of the Norwegian Geological Survey efforts to investigate the oceanic domain west of Svalbard and the western Barents Sea margin[16, 17]. The airborne data were acquired at 120 m above sea level and with a line spacing of 5500 m. The survey area extends 120 km in NW-SE and 150 km in SW-NE. It encompasses the eastern end the Mohns Ridge, the southern part of the Knipovich Ridge and the bend marking their junction (Fig. 3a).

2.2) Magnetic Exploration Of The Ridges Junction

The near-seafloor magnetic data reveal a significant drop in the equivalent magnetization while the AUV passes between the hydrothermal mounds (Fig. 2a, b). Logically, the RTP magnetic anomaly and the vertical derivative also indicate that the site is associated with a negative RTP magnetic anomaly, confirming previous studies and proving that this hydrothermal site sits on a basaltic substratum[9] (Fig. 2c, d).

Regional magnetic data display long-wavelength magnetic anomalies corresponding, among others, to the inversions of the geomagnetic field polarity. The amplitude of these anomalies decreases while moving away from the spreading axis, as the basalt gets progressively altered by seawater circulation. The off-axis bathymetric Hill A is located on both sides of the Gauss-Gilbert geomagnetic polarity reversal, and is therefore associated with a magnetization switching from positive to negative polarities while moving off axis. Unsurprisingly, the prominent Hill A induces a magnetic anomaly with a higher amplitude than the surroundings (Fig. 3).

2.3) Observations

Oceanic Core Complexes exclusively form along slow and ultraslow-spreading centers, i.e., in dominantly tectonic environments[7, 18, 19], and preferentially develop near the end of ridge segments[8]. In their strict definition, these structures correspond to oceanic massifs constituted by mafic plutons and/or ultramafic mantle rocks that exhume on the seafloor, at the footwall of low-angle detachments[20].

As imaged by seismic data, OCCs detachment faults show gentle and smooth convex upward profile[21, 22] and often develop corrugated dome-like structures with striations parallel to the displacement direction[21–23]. Meanwhile, the hanging wall of the detachment often corresponds to graben-type structures, including a conjugate pattern of steep normal faults[8, 24]. Deformation of the footwall rocks in the detachment zone is localized within a narrow shear zone (< 200 m)[25]. During the spreading, the space created by footwall rotation is progressively accommodated by addition of hot viscous magmas at the root of the detachment and/or flow of the ductile mantle[25]. On the basis of observations and modelling, a rolling hinge mechanism involving progressive unroofing and denudation of the mantle has been widely accepted for the development of OCCs[26].

Being a slow-spreading center, the Mohns Ridge could constitute a preferential area for the development of such mantle exposures, particularly near its junction with the Knipovich Ridge. As a result, the prominent Hill A located 30 km to the Northwest of the ridge axis was previously classified as an OCC[27, 28] (Fig. 1a). The main argument for an OCC interpretation was the collection of two rock samples containing gabbros and serpentinites in its surroundings[9, 29, 30]. Nevertheless, bathymetric and magnetic observations suggest that despite the presence of these rocks, this bathymetric high does not match the characteristics of true OCCs.

The presence of serpentinites near the end of slow-spreading segments is common[8], but does not necessarily imply the existence of OCCs[5, 6, 31]. The recovered mafic grab-samples do not come from the controversial hill, but were instead collected either between the neovolcanic zone and its foot or on another hill, located 25 km further south[29] (Fig. 3a). These rocks therefore do not address the question of the hill geology, and do not confirm the presence of a mafic massif on its top.

Compared to confirmed OCCs, the Hill A does not clearly show any smooth and corrugated morphology, as expected in response to a rolling hinge denudation of potential mantle rocks. The seafloor ruggedness

instead suggests the presence of numerous and widely distributed steep normal faults from the rift valley up to the elevated flanking terrain. Despite a marked prominence, the bathymetry underlines that the structural style does not differ from the surrounding basaltic seafloor (Fig. 3b).

To obtain a quantitative support, we considered and modeled two magmato-tectonic scenarios:

1. The Hill A is dominantly basaltic. This scenario aligns with the off-axis basaltic seafloor confirmed from the high-resolution magnetic data collected over hydrothermal site Loki's Castle. Assuming this hypothesis, the average magnetization of the rock constituting the hill should be consistent with the surrounding basaltic seafloor at a comparable distance from the spreading axis. In this context, the few recovered rock samples would originate from small mantle pocket exposures typically found near the end of ridge segments[32]. We compare the data along Profile 1 with another profile (Profile 2) located further southwest, where no mantle rocks exposure has been found. The quantification and removal of the hill's magnetic footprint confirm that the seafloor along both profiles have comparable magnetic signatures (Methods) and should be of similar geology (i.e., basaltic) (Fig. 3b).
2. The Hill A is dominantly ultramafic. Such alternative scenario would support the existence of an OCC. With such a crustal configuration, we would expect the rock absolute magnetization on top of the hill to be approximately five times weaker than that of the basalt[33, 34]. Under these constraints, preserving the observed RTP magnetic anomaly amplitude implies an accumulation of magnetized material considerably more important than for a basaltic layer. It would require an unrealistically tall bathymetric feature, which is inconsistent with present-day observations and the inversion results (Methods).

The formation of OCCs is usually associated with a marked asymmetry in the regional magnetic anomalies, as the spreading essentially occurs on one side of the ridge axis[35]. However, no significant asymmetry in the geomagnetic polarity reversals is observed[16] in the vicinity of Mohns and Knipovich Ridges junction and no evidence suggests that the spreading occurred exclusively on the northwestern side of the spreading axis (Fig. 3a). The regional magnetic anomalies and the modeling support our idea and suggest that no major unroofing from the deep crust and upper mantle denudation is at play.

3) Discussion

Our observations and modelling result concur with the idea that the off-axis prominent bathymetric Hill A should be considered a distinct mega-abyssal hill, differing from those commonly found on the flanks of slow-spreading ridges[36]. Hill A does not match the characteristics of a true OCC either, in contrast with previous assumptions[27, 28]. The uplifted terrain observed west of the Mohns ridge valley could have formed by voluminous basaltic eruptions along fissure swarms, even if the origin of this magmatic impulse remains unclear. Alternatively, the western elevated terrain could have formed amagmatically by flexural response. The basement peak on the western flank of the axial valley could have been caused by flexural response to the mass redistribution triggered by the normal faulting[37]. The basement shape of the abyssal hill observed close to magnetic chrons C2A[16] qualitatively resembles what would be

expected from the flexure of a lithosphere with an effective elastic thickness of the order of 5 km, not unusual for young oceanic lithosphere[37]. The main high could be similar to the "inside corner hogback" structure observed in the bend of the aborted Aegir Ridge, in the Norway Basin[38], but has never been documented along active ridge. To form the elevated high in this manner, the total slip along the normal faults bounding the Mohns and Knipovich Ridges could have been sufficient to create an atypical and mechanical elevation with or without excess magmatism. However, magnetic considerations and modelling suggest that flexure uplift was probably not sufficient to cause the fault scarps to curve enough to develop a rolling hinge process and ultimately severe unroofing of the oceanic mantle. This "structural cousin of OCC"[38], or Proto-Core Complex (PCC), might have evolved into a real one, had fault motion continued (Fig. 4). It may represent a different class of oceanic structures, pointing toward a significantly more diverse seafloor geology than expected in the vicinity of slow-spreading centers, and directly related to the level of spreading asymmetry. Finally, magnetic constraints and a dedicated modeling approach and methodology remain fundamental requirements to clarify and differentiate the two classes of abyssal highs.

4) Methods

The method to resolve magnetic anomalies from the raw data has already been documented in various articles[39, 40] and is included in the Supplementary Information. Here we describe the further data processing steps through various magnetic inversion methods, and the magnetic model used to assess the geology of the discussed bathymetric hill.

4.1) Magnetic Inversions

High-resolution magnetic data were inverted into equivalent magnetization using a specifically designed method[10]. For the regional magnetic data, we have widened the use of this method and also applied a more common one[41], to achieve various levels of resolution. In all cases, a mathematically rigorous Reduced-to-the-Pole (RTP) magnetic anomaly was computed using the equivalent magnetization models and assuming a vertical geomagnetic field.

Unlike other methods, the Bayesian inversion[10] does not require any filtering, i.e., it preserves the entire signal wavelength content. It was the only solution to clearly display the lack of magnetization associated with the hydrothermal site Loki’s Castle, confirming the basaltic nature of the substratum.

It should be noted that the roughly circular shape of the reduced equivalent magnetization and the corresponding RTP magnetic anomaly cannot be considered as depicting the contours of the area affected by hydrothermal circulation, as a single AUV route passes between the two mounds. This shape results from gridding effects and its spatial extension cannot be delineated with this dataset. We therefore insist on the fact that our goal here is to confirm the basaltic nature of the substratum and not to study the hydrothermal site itself.

On regional magnetic data, the results from the two inversion methods[10, 41] reveal that the Bayesian inversion allows a significant gain in terms of wavelength content (Supplementary Fig. 1). Nevertheless, this gain also leads to a paradoxical situation where the geomagnetic inversions become more difficult to identify because the lack of filtering results in the short wavelengths of the signal to partially hide them.

The RTP magnetic anomalies have been computed using these two approaches. The one derived from the Bayesian inversion logically displays a richer frequency content (Supplementary Fig. 1), and the difference with the RTP magnetic anomaly computed from the Parker and Huestis method[41] reveals that all wavelengths shorter than 5 km are absent from this second approach. By comparing these two different approaches, it becomes possible to:

1. Precisely delineate the geomagnetic polarity reversals thanks to the Parker and Huestis method and associated RTP magnetic anomaly to avoid the risk of data misinterpretation. Such delineation reveals that no significant magnetic asymmetry exists on the regional magnetic data and that the discussed off-axis prominent bathymetric feature sits on both sides of the Gauss/Gilbert polarity reversal.
2. Quantify and study the magnetic response of the controversial Hill A and to rule out the previously mentioned OCC hypothesis, suggesting a more peculiar and complex geological history.

4.2) Forward Modeling Approach

Along the profile cutting across the ridge axis, the hydrothermal site Loki's Castle and the discussed Hill A, a magnetic model has been computed. This model consisted of artificially removing the presence of the Hill A and comparing the result with the observed RTP magnetic anomaly along the second profile, where no such hill appears. The bathymetry has been discretized into prisms with a 100x100 m square section and a 5 km depth, identical to the magnetized layer thickness chosen to perform the inversions. The prisms are associated with the magnetization obtained from the inversions and those constituting the Hill have been removed from the data. Instead, an artificial, flatter surface fills the gap. This surface is comparable to the seafloor morphology along the second profile at similar distance from the ridge axis. Prisms located within this surface are associated with the magnetization resulting from the inversion. A model is computed in the geometry of the experiment, assuming a vertical geomagnetic field. The difference between synthetic (purple line on Fig. 3b) and observed magnetic anomaly on the Hill A corresponds to the magnetic footprint of the Hill. The magnetic model without the Hill A can finally be compared to the observed magnetic anomaly along Profile 2 to assess the seafloor geology.

Declarations

Competing Interests statement

The authors declare no competing interests.

Acknowledgements

We thank the captain and crew of the R/V *Polar King* for excellent work at sea. We also thank the AUV *Hugin* engineering team for their technical expertise. This research was financially supported by the Geological Survey of Norway (NGU, Trondheim, Norway).

Author contributions

F. S. processed and interpreted the data and wrote the article. L. G. brought his expertise regarding the tectonic phenomena at play within the Mohns and Knipovich Ridges and contributed to refine the interpretations. A. L. provided the high-resolution magnetic data over hydrothermal site Loki's Castle and contributed to their interpretations. M. B. contributed to interpret the data.

References

1. Talwani, M. & Eldholm, O. Evolution of the Norwegian-Greenland Sea. *GSA Bulletin* **88** (7), 969-999 (1977). https://doi.org/10.1130/0016-7606(1977)88<969:EOTNS>2.0. CO;2.
2. Eldholm, O., Karasik, A. M. & Reknes, P. A. The North American plate boundary in: Grantz A., L. Johnson, and J. F. Sweeney, (Eds.), The Arctic Ocean Region. The Geology of North America. *Geological Society of America, Boulder, Colorado*, 171-184.
3. De Mets, C., Gordon, R. G., Argus, D. F. & Stein, S. Current plate motions. *Geophys. J. Int.***101**, 425-478 (1990).
4. Torsvik, T. H., Mosar, J. & Eide, E. A. Cretaceous-Tertiary geodynamics: a North Atlantic exercise. *Geophys. J. Intern.* **146**, 850-866 (2001).
5. Dick, H., Lin, J. & Schouten, H. An ultraslow-spreading class of ocean ridge. *Nature* **426**, 405-412 (2003).
6. Cannat, M. Emplacement of mantle rocks in the seafloor at mid-ocean ridges. *J. Geophys. Res.* **98**, 4163-4172 (1993). doi:10.1029 /92JB02221.
7. Tucholke, B. E., Lin, J. & Kleinrock, M. C. Megamullions and mullion structure defining oceanic metamorphic core complexes on the Mid-Atlantic Ridge. *J. Geophys. Res.* **103**, 9857-9866 (1998). doi:10 .1029/98JB00167.
8. Escartín, J., et al. Central role of detachment faults in accretion of slow-spreading oceanic lithosphere. *Nature* **455**, 790-794 (2008). doi:10.1038 /nature07333.
9. Pedersen, R. B., Thorseth, I. H., Nygård, T. E., Lilley, M. D. & Kelley, D. S. Hydrothermal activity at the Arctic mid-ocean ridges, in: Rona, P. A., Devey, C. W., Dyment, J., Murton, B. J. (Eds.). *Geophysical Monograph Series. American Geophysical Union*, Washington, D. C., 67-89 (2010).
10. Honsho, C., Ura, T. & Tamaki, K. The inversion of deep-sea magnetic anomalies using Akaike's Bayesian information criterion. *J. Geophys. Res.* **117** (2012). doi:10.1029/2011JB008611.
11. The Mareano project. https://www.mareano.no/en/maps-and-data/marine-geospatial-data. The Norwegian Mapping Authority, Hydrographic Service (2019).

12. Riley, S. J., DeGloria, S. D. & Elliot, R. A terrain ruggedness index that quantifies topographic heterogeneity. *Intermountain Journal of Sciences* **5**, 1-4 (1999).
13. Peyve, A. A., et al. The structure of the Knipovich-Mohns junction (North Atlantic). *Dokl. Earth. Sc.* **426**, 551-555 (2009). https://doi.org/10.1134/S1028334X09040096.
14. Ludvingsen, M. et al. MarMine Cruise Report – Arctic Mid-Ocean Ridge 15.08.2016 - 05.09.2016; NTNU; Trondheim, Norway (2016).
15. Lim, A., Brönner, M., Johansen, S. E. & Dumais, M. A. Hydrothermal activity at the ultraslow-spreading Mohns Ridge: New insights from near-seafloor magnetics. *Geochem. Geophys. Geosyst.* **20** (2019). https://doi.org/10.1029/2019GC008439.
16. Novatem, Knipovich Ridge airborne survey 2016 (KRAS-16) -Technical Report, 32pp pp. Oakey, G. N., & Chalmers, J. A. (2012). A new model for the Paleogene motion of Greenland relative to North America: Plate reconstructions of the Davis Strait and Nares Strait regions between Canada and Greenland. *J. Geophys. Res.* **117** (B10) (2018).
17. Dumais M. A., Gernigon, L., Olesen, O., Johansen, S. E. & Brönner, M. New interpretation of the spreading evolution of the Knipovich Ridge derived from aeromagnetic data. *Geophys. J. Int.* **224** (2), 1422-1428 (2021).
18. Cann, J. R., et al. Corrugated slip surfaces formed at North Atlantic ridge-transform intersections. *Nature* **385**, 329-332 (1997).
19. Tucholke, B. E., Behn, M. D., Buck, W. R. & Lin, J. Role of melt supply in oceanic detachment faulting and formation of megamullions. *Geology* **36**, 455-458 (2008). doi:10.1130/G24639A.
20. Searle, R. Mid-Ocean Ridges. *University Printing House, Cambridge CB2 8BS, United Kingdom*. Published in the United States of America by Cambridge University Press, New York (2013).
21. Ranero C. R. & Reston, T. J. Detachment faulting at ocean core complexes. *Geology* **27**, 983-986, (1999).
22. Blackman, D. K., Canales, J. P., Harding, A. Geophysical signatures of oceanic core complexes. *Geophys. J. Int.* **178** (2), 593-613 (2009). https://doi.org/10.1111/j.1365-246X.2009.04184.x.
23. Sauter, D. et al. Continuous exhumation of mantle-derived rocks at the Southwest Indian Ridge for 11 million years. *Nat. Geosci.* **6**, 314-320 (2013).
24. Canales, J. P., Tucholke, B. E. & Collins, J. A. Seismic reflection imaging of an oceanic detachment fault: Atlantis megamullion (Mid-Atlantic Ridge, 30°10'N). *Earth Planet. Sci. Lett.* **222**, 543-560 (2004). doi:10.1016/j.epsl.2004.02.023.
25. Escartin, J., Mével, C., MacLeod, C. J. & MacCaig A. M. Constraints on deformation conditions and the origin of oceanic detachments: The Mid-Atlantic Ridge core complex at 15°45'N. *Geochem. Geophys. Geosyst.* **4** (8) (2003). doi:10.1029/ 2002GC000472.
26. Lavier, L. L., Buck, W. R. & Poliakov, A. N. B. Self-consistent rolling hinge model for the evolution of large-offset low-angle normal faults. *Geology* **27** (12), 1127-1130 (1999).

27. Whitney, D. L., Teyssier, C., Rey, P. F. & Buck, R. Continent and Oceanic Core Complexes. *GSA Bulletin* **125** (3-4), 273-298 (2013).
28. Reimers, H. Identifying oceanic core complexes and associated detachment faulting on the ultraslow spreading Mohns Ridge and links to SMS deposits. *Mineralproduksjon* **9**, A25-A53 (2020).
29. Pedersen, R. B., et al.. Hydrothermal activity and core complex formation at the Arctic Mid-Ocean Ridge: An overview of preliminary results of the H2DEEP expedition to the southern Knipovich Ridge at 73N. *Amercian Geophysical Union, Fall Meeting, Abstract #OS41C-05*, 5-7 (2007).
30. Cruz, M., A. et al. Geochemistry of the Artic Loki's Castle hydrothermal vent products. *In Proceedings of the Goldschmidt Conference*, Prague, Czech Republic (2011).
31. Cannat M. & Casey, J. F. An ultramafic lift at the Mid-Atlantic Ridge: Successive stages of magmatism in serpentinized peridotites from the 15°N region, in mantle and lower crust exposed in oceanic ridges and in ophiolites. *Edited by R. L. M. Vissers and A. Nicolas*, 5-34 (1995).
32. Cannat, M., et al. Thin crust, ultramafic exposures, and rugged faulting patterns at the Mid-Atlantic Ridge (22°-24°N). *Geology* **23** (1), 49-52. (1995). doi: https://doi.org/10.1130/0091-7613(1995)023<0049:TCUEAR>2.3.CO;2.
33. Szitkar, F., Dyment, J., Fouquet, Y., Honsho, C. & Horen, H. The magnetic signature of ultramafic-hosted hydrothermal sites. *Geology* **42**, 715-718 (2014).
34. Szitkar, F., Dyment, J., Fouquet, Y., Choi, Y. & Honsho, C. Absolute magnetization of the seafloor at a basalt-hosted hydrothermal site: insights from a deep-sea submersible survey. *Geophys. Res. Lett.* **42** (2015). doi: 10.1002/2014GL062 791.
35. Searle, R. C., MacLeod, C. J., Peirce, C. & Reston, T. J. The Mid-Atlantic near 13°20'N: High-resolution magnetic and bathymetry imaging. *Geochem. Geophys. Geosyst.* **20**, 295-313 (2019). https://doi.org/10.1029/2018GC007940.
36. Behn, M. D. & Ito, G. Magmatic and tectonic extension at mid-ocean ridges: 1. Controls on fault characteristics. *Geochem. Geophys. Geosyst.* **9**, Q08O10 (2008). doi:10.1029/2008GC001965.
37. Weissel, J. K. & Kamer, G. D. Flexural uplift of rift flanks due to mechanical unloading of the lithosphere during extension. *J. Geophys. Res.* **94**, 13919-13950 (1989).
38. Vogt, P. R. & Jung, W. Y. Treitel Ridge: a unique inside corner hogback on the west flank of extinct Aegir spreading ridge, Norway Basin. *Mar. Geol.* **267**, 86-100 (2009).
39. Honsho, C., et al. Magnetic structure of a slow-spreading ridge segment: Insight from near-bottom magnetic measurements onboard a submersible. *J. Geophys. Res.* **114**, B05101, (2009). doi:10.1029/2008JB005915.
40. Isezaki, N. A new shipboard three-component magnetometer. *Geophysics* **51**, 1992-1998 (1986).
41. Parker, R. L. & Huestis, S. P. The inversion of magnetic anomalies in the presence of topography. *J. Geophys. Res.* **79**, 1587-1593 (1974).

Figures

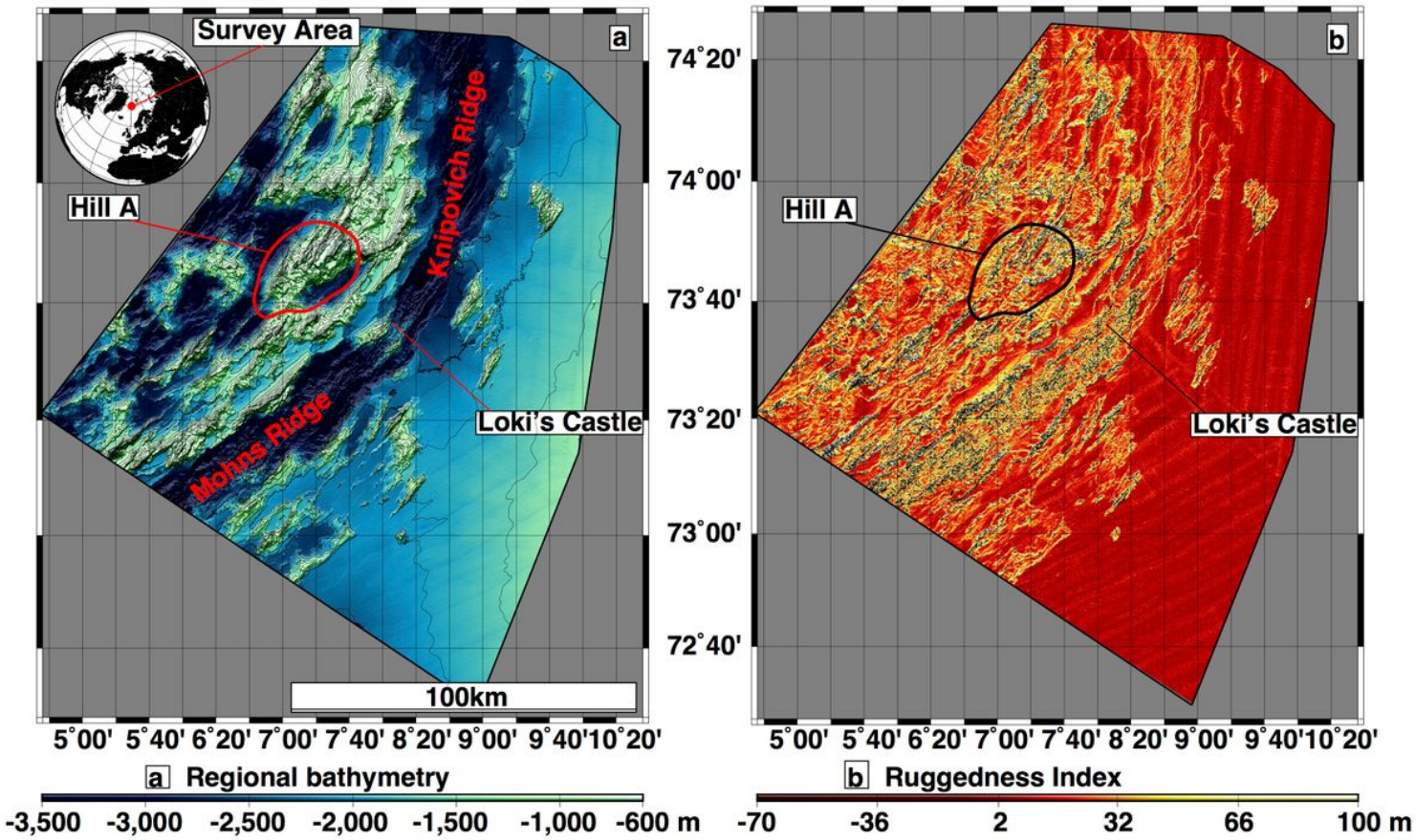

Figure 1

General overview of the survey area. (a) Regional bathymetry of the junction between the Mohns and the Knipovich Ridges. The bend in the spreading axis direction is clearly visible. (b) Ruggedness map of the area underlining the similar morphologies between the controversial Hill A and the surrounding basaltic terrain.

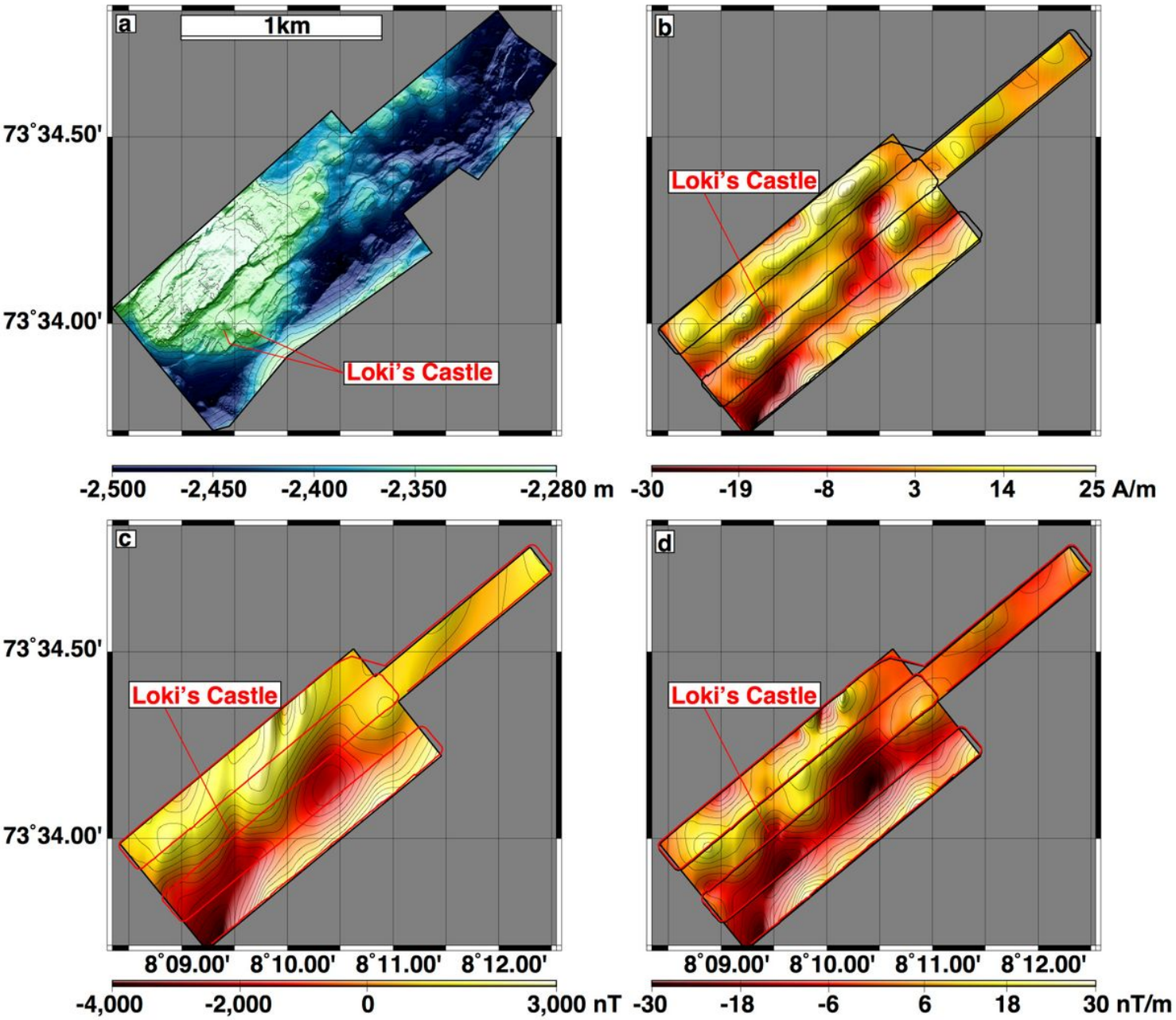

Figure 2

Magnetic signature of hydrothermal site Loki's Castle. (a) High-resolution magnetic anomaly measured by the AUV Hugin over basalt-hosted hydrothermal site Loki's Castle. (a) High-resolution bathymetry over active, basalt-hosted hydrothermal site Loki's Castle. (b) Equivalent magnetization obtained using Honsho's Bayesian inversion(10). A clear drop in the signal appears when the AUV passes between the hydrothermal mounds, confirming that the site sits on a basaltic substratum. (c) RTP magnetic anomaly computed from the Bayesian inversion. The site is associated with a distinct magnetic signature. (d) Vertical derivative of the RTP magnetic anomaly. The drop visible on (b), (c) and (d) confirms the basaltic nature of the substratum supporting the site.

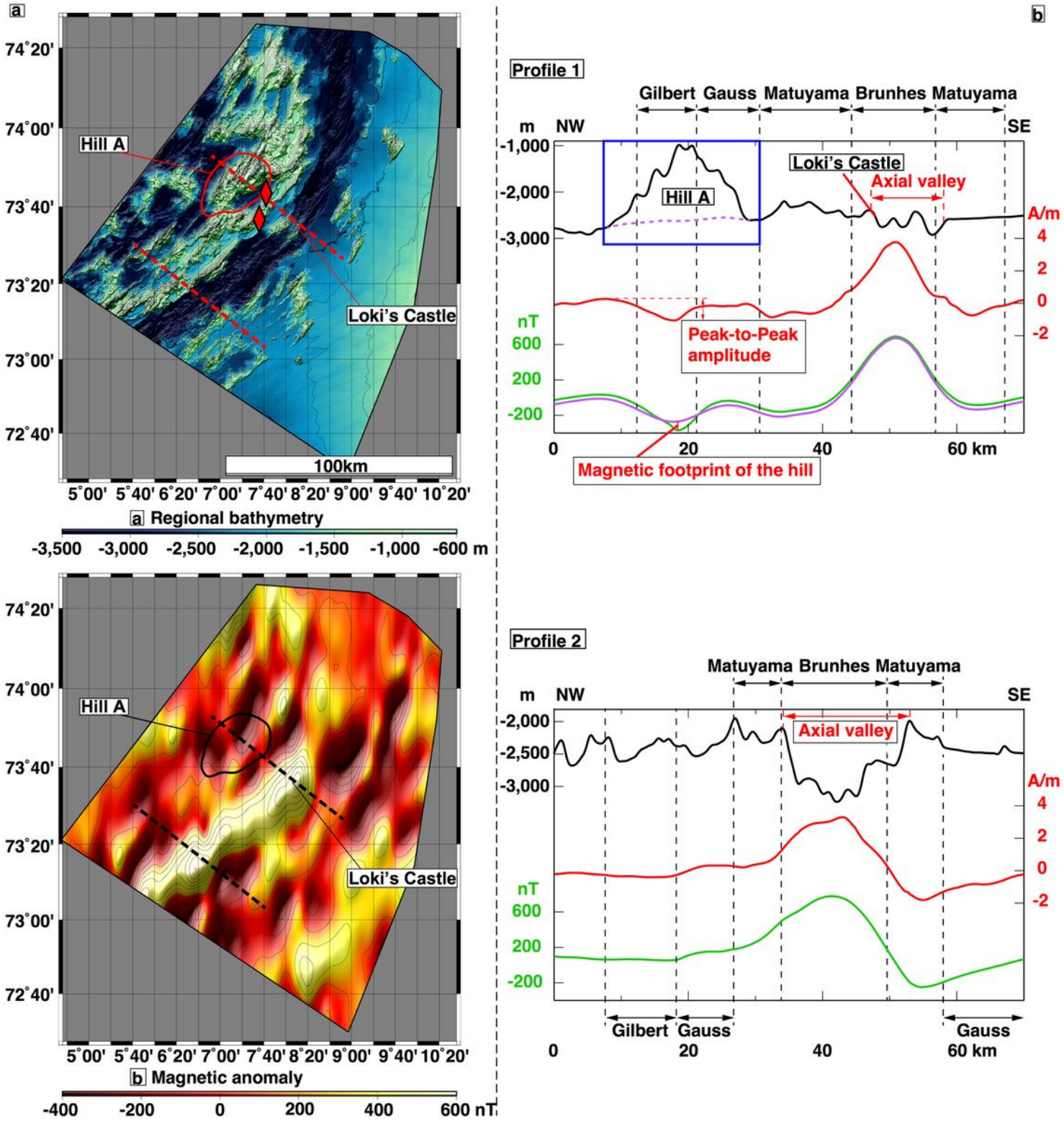

Figure 3

Morphology and geophysical response of the controversial Hill A. (a) (Top) Regional bathymetry. The bathymetric high displays a typical basaltic seafloor roughness. Red diamonds correspond to the places where rock samples containing gabbro and serpentinite were recovered(9). (Bottom) Magnetic anomalies showing the reversals in the geomagnetic field polarity. No clear asymmetry appears on the magnetic anomalies in the vicinity of the bend, suggesting that the spreading did not exclusively occurred on the

northwestern side of the ridge axis. (b) (Top) Profile 1 across the mid-ocean ridge axis, the basalt-hosted hydrothermal site Loki's Castle and the Hill A. The equivalent magnetization (red line) does not suggest any change in geology of the seafloor between the ridge axis and the bathymetric high. The RTP anomaly (green line) confirms the progressive alteration of the terrain while moving off axis. The Hill A is associated with a peak-to-peak magnetic anomaly twice bigger than other bathymetric structures located closer to the ridge axis. A magnetic model without the bathymetric high (purple line) confirms the impact of this accumulation of magnetized material and suggests that a weakly magnetized OCC could not generate such of amplitude. (Bottom) Profile 2, with an orientation parallel to Profile 1. This control profile cuts across basaltic terrain exclusively. The equivalent magnetization and RTP magnetic anomalies have an amplitude consistent with those observed along Profile 1, confirming that the geology is comparable.

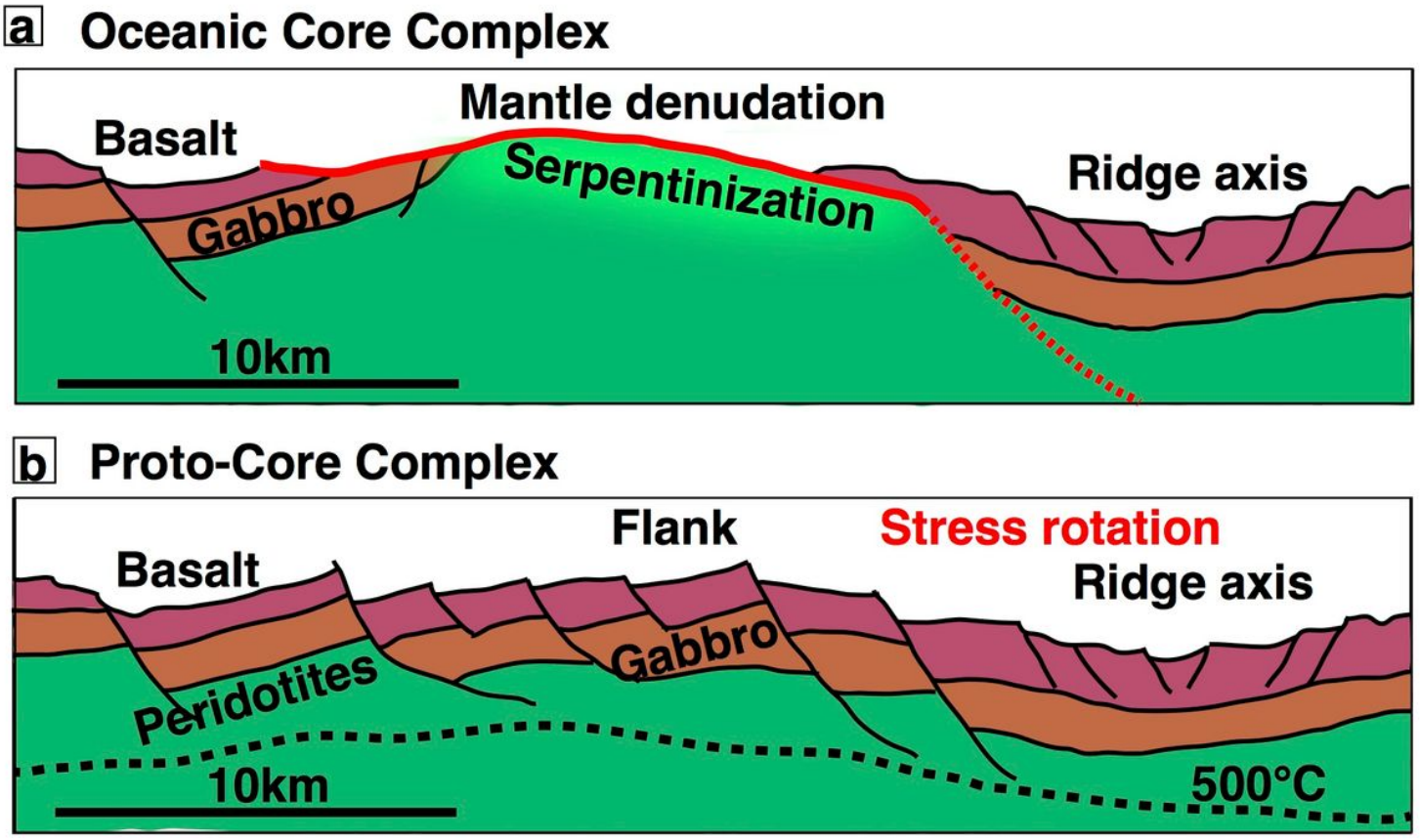

Figure 4

Diagram illustrating the impact of spreading asymmetry on seafloor geology. (a) Fully developed Oceanic Core Complex. A complete spreading asymmetry results in a denudation of the mantle. (b) Partial spreading asymmetry comparable to what happens ner the bend marking the junction between the Mohns and the Knipovich Ridges. An off axis appears however the fault motion was not sufficient to allow the formation of an Oceanic Core Complex, resulting in the development of a Proto-Core Complex.

Supplementary Files

This is a list of supplementary files associated with this preprint. Click to download.

- Supplementary.docx
- SupplementaryFigure1.jpg